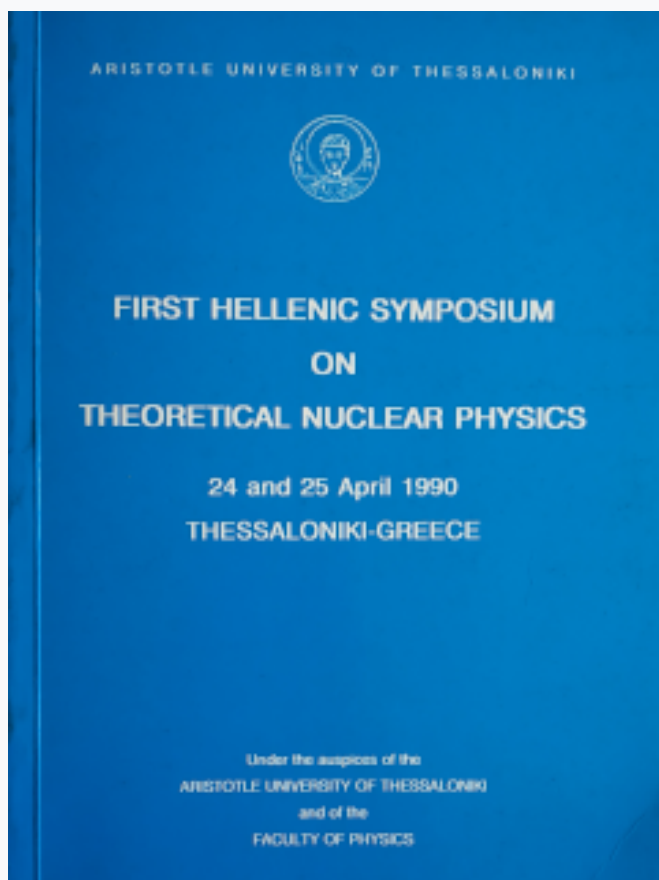


## HNPS Advances in Nuclear Physics

Vol 1 (1990)

HNPS1990



### Shell model calculations in the A=80-100 mass region and study of double $\beta$ transitions

*J. Sinatkas, L. D. Skouras, D. Strottman, J. D. Vergados*

doi: [10.12681/hnps.2834](https://doi.org/10.12681/hnps.2834)

#### To cite this article:

Sinatkas, J., Skouras, L. D., Strottman, D., & Vergados, J. D. (2020). Shell model calculations in the A=80-100 mass region and study of double  $\beta$  transitions. *HNPS Advances in Nuclear Physics*, 1, 156–167.  
<https://doi.org/10.12681/hnps.2834>

## Shell model calculations in the $A = 80 - 100$ mass region and study of double $\beta$ transitions<sup>1</sup>

J. Sinatkas<sup>1</sup>, L.D. Skouras<sup>1</sup>, D. Strottman<sup>2</sup> and J.D. Vergados<sup>3</sup>

<sup>1</sup> Institute of Nuclear Physics, N.C.S.R. *Demokritos* Aghia Paraskevi GR 15310, Greece

<sup>2</sup>T2 group, Los Alamos National Laboratory Los Alamos, New Mexico, USA

<sup>3</sup>Physics Department, The University of Ioannina GR 45338 Ioannina, Greece

**Abstract:** The structure of the  $Z, N \leq 50$  nuclei is examined in a model space consisting of the  $0g_{9/2}$ ,  $1p_{1/2}$ ,  $1p_{3/2}$  and the  $0f_{5/2}$  hole orbitals outside the doubly closed  $^{100}_{50}\text{Sn}$  core. The effective interaction for this model space is derived by introducing second order corrections to the Sussex matrix elements, while the one-hole energies are deduced by a least square fit to the observed levels. The results of the calculation are found to be in very satisfactory agreement with experiment for all nuclei with  $38 < Z \leq 46$  but for  $Z \leq 38$  this agreement begins to deteriorate. Such a feature possibly indicates the appearance of deformation and the breaking of the  $N = 50$  core. The wavefunctions of the calculation are used to determine double  $\beta$  matrix elements in the Ge, Se, Sr and Kr isotopes.

### 1. Introduction

In this paper we present the results of two recent shell-model calculations<sup>1,2)</sup> on the structure of nuclei with  $Z, N \leq 50$ , where  $Z$  and  $N$  denote proton and neutron numbers, respectively. In these calculations we employ a model that is capable, in principle, to describe all nuclei with  $28 \leq Z, N \leq 50$ . In this model the doubly closed  $^{100}_{50}\text{Sn}$  is considered as an inert core and the nuclei under consideration are described in terms of proton and neutron holes occupying the  $0g_{9/2}$ ,  $1p_{1/2}$ ,  $1p_{3/2}$  and  $0f_{5/2}$  orbitals of the harmonic oscillator potential.

Previous shell-model studies of the  $Z, N \leq 50$  nuclei<sup>3-11)</sup> assumed a  $^{88}_{38}\text{Sr}$  core and placed the proton particles and neutron holes in the  $0g_{9/2}$  and  $0p_{1/2}$  orbitals.

---

<sup>1</sup>Presented by J. Sinatkas

In these calculations the matrix elements of the effective hamiltonian and transition operators were treated as parameters which were deduced by a least square fit to the experimental data. Despite the success these calculations had in accounting for many of the observed properties of nuclei with  $Z > 38$  and  $N = 50 - 48$ , a direct comparison with experiment<sup>12)</sup> reveals that certain low-lying states of these nuclei cannot be accounted for in the small  $g9/2, p1/2$  space. In addition, the study of the double-beta transitions in Kr, Se and Ge nuclei, which is a problem that attracts a lot of interest recently<sup>13)</sup>, can only be accomplished by the use of an extended shell-model space, like the one considered in the present calculation.

One of the problems faced with the use of the  $0g9/2, 1p1/2, 1p3/2$  and  $0f5/2$  space is that the energy matrices have very large dimensions. This problem, which is already serious for the  $N = 50$  nuclei, becomes forbidding in the case of the  $N < 50$  nuclei unless a suitable truncation scheme is introduced. This truncation scheme with other details of the calculation are described in sect. 2, while the results of the calculation are presented in sect. 3.

## 2. Details of the calculation

In this section we describe the shell-model calculations by which we determined the properties of the  $Z, N \leq 50$  nuclei.

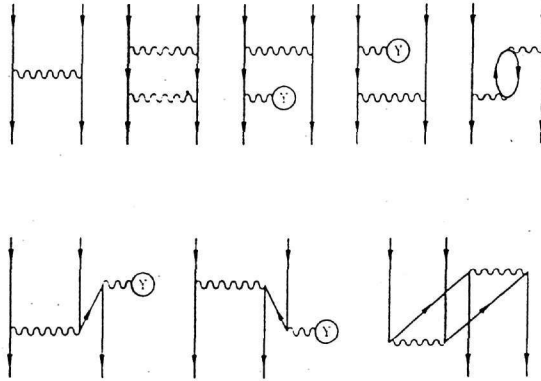


Figure 1: Diagrams considered in the determination of the two-hole effective interaction.

In our calculations the doubly closed nucleus  $^{100}_{50}\text{Sn}$  is assumed as an inert core and the nuclei under consideration are described in terms of proton and neutron holes that

are distributed in the  $0g9/2$ ,  $1p1/2$ ,  $1p3/2$  and  $0f5/2$  orbitals. This choice of model space has the advantage that protons and neutrons are treated on equal basis. The determination of the effective hamiltonian, that is appropriate to our choice of model space, has been described in detail in Refs 1-2 so only its main features need to be mentioned here. Thus the two-body interaction has been determined by considering all second order diagrams, examples of which are shown in fig. 1, in the space of  $4\hbar\omega$  excitations and using the *Sussex*<sup>14)</sup> interaction as a  $G$  matrix. In addition the hamiltonian contains six parameters that were determined by a least square fit to the energy spectra of a wide range of nuclei. Three of these parameters correspond to the one-hole energy of the  $1p1/2$ ,  $1p3/2$  and  $0f5/2$  orbitals relative to the  $0g9/2$ . These energies cannot be taken directly from experiment since the one-hole nuclei  $^{99}_{50}\text{Sn}$ ,  $^{99}_{49}\text{In}$  are far from the stability line and their spectra have not yet been observed. The values determined by a least square fit to the energy spectra of nuclei with  $N = 50$  and  $37 \leq Z \leq 44$  are given by:

$$\epsilon_{9/2} = 0, \quad \epsilon_{1/2} = 1.85, \quad \epsilon_{3/2} = 3.45, \quad \epsilon_{5/2} = 6.32 \quad (1)$$

The other three parameters, which are denoted by  $x_1$ ,  $x_2$  and  $x_3$ , multiply the matrix elements of the types  $\langle 9/2, 1/2; JT = 0 | V | 9/2, 1/2; JT = 0 \rangle$ ,  $\langle 9/2, 1/2; JT = 0 | V | 9/2, 3/2; JT = 0 \rangle$ ,  $\langle 9/2, 3/2; JT = 0 | V | 9/2, 3/2; JT = 0 \rangle$  thus modifying their strength from that determined by second order perturbation theory. The values of these three multiplicative factors have been determined by a least square fit to the energy of 40 levels of the  $N = 49, 48$  nuclei. The values obtained from this procedure are given by:

$$x_1 = 0.68, \quad x_2 = 0.66, \quad x_3 = 0.88 \quad (2)$$

In a similar manner to the perturbative determination of the effective interaction, we have also determined matrix elements of effective transition operators. As an example of this calculation we list in table 1 the reduced matrix elements corresponding to single-proton hole states. Table 1 also includes the values corresponding to the bare operators so that one can obtain an estimate of the corrections. As the results of table 1 indicate, these corrections are both sizable and also state-dependent.

The large number of valence holes (24 in the case of  $^{76}\text{Ge}$ ) together with the number of orbitals involved in the model space combine to produce exceedingly large dimensions for the energy matrices. For this reason the weak-coupling approximation has been adopted. Thus the total hamiltonian is conveniently expressed as

$$H = H_\pi + H_\nu + V_{\pi\nu} \quad (3)$$

where  $H_\pi$  and  $H_\nu$  describe the effective hamiltonian in the proton and neutron spaces, respectively, while  $V_{\pi\nu}$  denotes the effective interaction between proton and neutron

**Table 1**  
Reduced matrix elements  $\langle j_1^{-1} || T^L || j_2^{-1} \rangle^\dagger$   
for proton holes in the  $g9/2, p1/2, p3/2, f5/2$  space

$T^L$	$2j_1$	$2j_2$	Bare	Effect.
$M1$	9	9	11.598	10.322
	1	1	-0.3151	-0.0933
	1	3	2.5838	1.6520
	3	3	4.7811	3.8455
	3	5	0	0.1163
	5	5	1.2241	2.2278
$E2$	9	9	23.822	36.234
	1	3	-11.196	-18.624
	1	5	11.402	19.674
	3	3	11.196	18.495
	3	5	6.0945	10.821
	5	5	14.659	24.832
$M2$	9	5	46.671	31.193
$E3$	9	3	-113.58	-200.48
	9	5	-41.100	-78.155
$M3$	9	9	-494.33	-469.12
	1	5	9.0051	-8.4129
	3	3	-293.35	-264.59
	3	5	31.406	16.996
	5	5	8.7064	-45.111
$E4$	9	9	-660.14	-1072.5
	3	5	-444.38	-826.40
	5	5	-307.93	-575.89
$M4$	9	1	-2037.8	-2175.3
	9	3	2081.1	2356.3
	9	5	-1224.6	-1141.1

$^\dagger$   $EL$  matrix elements are expressed in units of  $e(fm)^L$  while  $ML$  in units of  $\mu_\nu(fm)^{(L-1)}$

holes. Because of the equivalence of protons and neutrons in our model the eigenvectors of  $H_\pi$  and  $H_\nu$  both correspond to states of nuclei with  $N = 50$ . These eigenvectors are then combined to form the basis for the weak-coupling calculation. Thus the basis vectors for a nucleus with  $n_\pi$  proton holes and  $n_\nu$  neutron holes are expressed as  $|n_\pi \mu_\pi j_\pi, n_\nu \mu_\nu j_\nu; J\rangle$ , where  $|n \mu j\rangle$  denotes the  $\mu$ th eigenvectors of those having spin  $j$  of the  $N = 50$ ,  $Z = 50 - n$  nucleus.

The calculation shows that the off-diagonal matrix elements of  $V_{\pi\nu}$  between basis states  $|n_\pi \mu_\pi j_\pi, n_\nu \mu_\nu j_\nu; J\rangle$ , which differ significantly in their  $\mu_\pi$  and  $\mu_\nu$  values are generally small. Such a feature justifies the weak-coupling approximation and helps to keep the order of the energy matrices relatively small. Thus the largest matrix in our calculation did not exceed the dimension 2000.

### 3. Results of the calculation

In this section we present a selection of the results of our shell-model calculations on the  $Z, N \leq 50$  nuclei and compare them with the experimental data.

Fig. 2 shows the theoretical and experimental spectra of  $^{94}\text{Ru}$  and  $^{92}\text{Mo}$ . As this figure shows, up to an excitation of about 3.5 MeV there is satisfactory agreement between theory and experiment for both these nuclei. This agreement is more impressive for the positive parity states which, as fig. 2 shows, the calculation, generally, reproduces within 100 KeV of their observed energy. On the other hand, the agreement is less satisfactory for the negative parity states for which the calculation, again generally, produces excitation energies that are higher from the observed values by about 400-600 KeV. For excitations higher than 3.5 MeV a detailed comparison between experiment and theory becomes difficult due to the density of states and to the many uncertainties that still exist in the experimental spectra. However, as fig. 2 shows, the calculation reproduces satisfactorily the energies of the observed high spin states like the possible  $9^-$ ,  $10^+$ ,  $11^-$  and  $12^+$  of  $^{94}\text{Ru}$  and the corresponding  $9^-$  and  $11^-$  of  $^{92}\text{Mo}$ . In addition, the calculation accounts for the presence of all observed states above 3.5 MeV that have definite spin and parity although for some of them, like the third  $0^+$  state of  $^{92}\text{Mo}$ , there is a significant difference between observed and calculated excitation energy.

The spectra of  $^{90}\text{Zr}$  and  $^{88}\text{Sr}$  are shown in fig. 3. As may be seen in this figure, the calculation reproduces in a very satisfactory way the observed spectrum of  $^{90}\text{Zr}$ . The only exception to this agreement is the octupole  $3^-$  state at 2.75 MeV in the experimental spectrum which the calculation, predicts to be more than one MeV higher. Generally, this calculation, like other calculations before<sup>3-8</sup>), fails to account satisfactorily for the presence of the low-lying  $3^-$  states in the spectra of the even mass

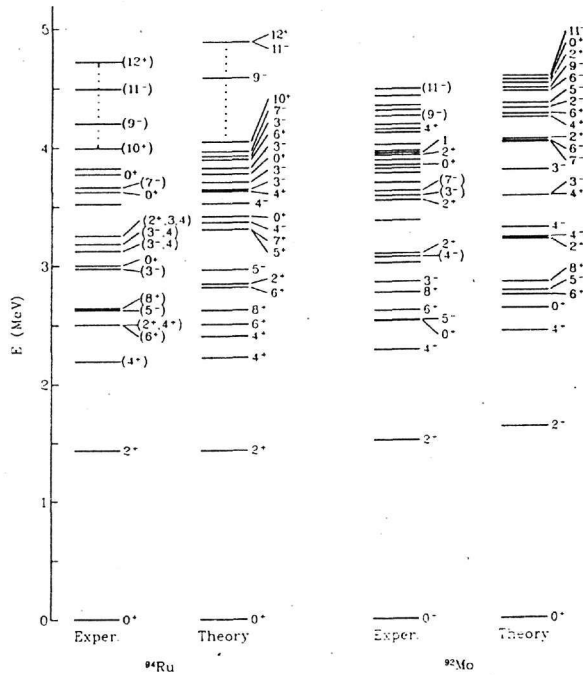


Figure 2: Theoretical and experimental spectra of  $^{94}\text{Ru}$  and  $^{92}\text{Mo}$

$N = 50$  nuclei. Such a feature strongly indicates the presence of strong admixtures of configurations outside the model-space in the wavefunctions of these states.

As fig. 3 shows, the calculation accounts for all the observed states of  $^{88}\text{Sr}$  up to about 4 MeV excitation. However in this case, unlike the case of  $^{90}\text{Zr}$  discussed above, the calculated excitation energies are not in very satisfactory agreement with the experimental ones. Thus, with the exception of the second  $0^+$  state, the theoretical levels appear to be between 400 and 700 KeV higher than the corresponding experimental states.

The failure of the calculation to explain satisfactorily the observed spectra of  $^{88}\text{Sr}$ , and also of other nuclei with  $Z < 38$ , can be attributed to the following two factors: i) To errors in the effective two-body interaction, and ii) To the presence of configurations outside the model space considered in the calculation.

As discussed in sect. 2, the effective two-hole interaction used in the present calculation contains few free parameters. Therefore, it is possible to improve the agreement with experiment by suitably adjusting more of the matrix elements of this

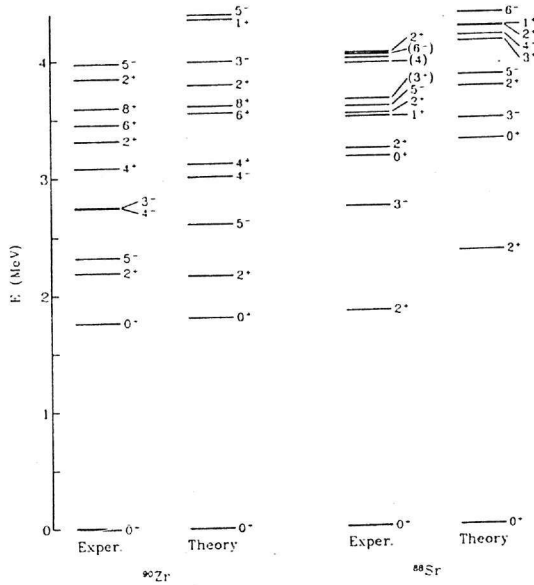


Figure 3: Theoretical and experimental spectra of  $^{90}\text{Zr}$  and  $^{88}\text{Sr}$

interaction. However, the application of such a method is difficult in the present case due to the many parameters involved ( 133 matrix elements) and to the many uncertainties that still exist in the experimental data.

As discussed above, the other possible reason for the failure of the present calculation to account satisfactorily for the observed spectra of  $^{88}\text{Sr}$  is due to the presence of configurations outside the model space in the low-lying states of these nuclei. The most probable such configurations are those that arise by breaking the  $N = 50$  core and exciting one or more neutrons to the  $0g7/2$ ,  $1d5/2$ ,  $1d3/2$ ,  $2s1/2$  and  $0h11/2$  orbitals of the empty shell above. The energy required for the breaking of the  $N = 50$  core can be compensated by the strong interaction between the proton and neutron holes. Of course, for such a situation to occur the number of proton holes must be large and such a requirement accounts for the fact that the disagreement between the present calculation and experiment begins to occur at  $^{88}\text{Sr}$ .

As a final example of the energy spectra obtained in our calculations<sup>2</sup>), we show



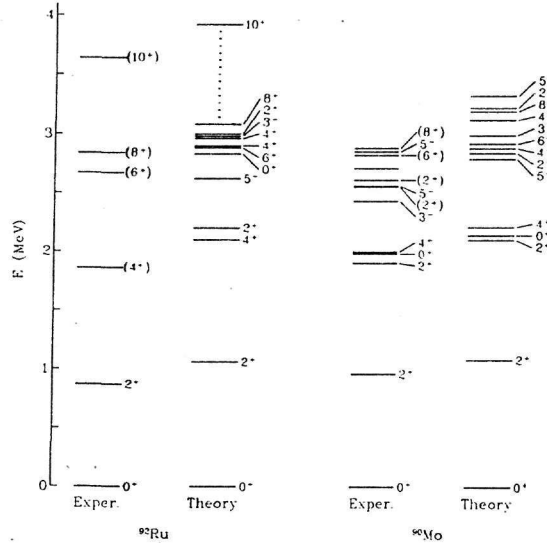


Figure 4: Theoretical and experimental spectra of  $^{92}\text{Ru}$  and  $^{90}\text{Mo}$

in fig. 4 the calculated energy scheme of the  $N = 48$  nuclei  $^{92}\text{Ru}$  and  $^{90}\text{Mo}$ . The experimental information on the first of these two nuclei is still very limited. As fig. 4 shows, the calculation accounts satisfactorily for all the observed states of  $^{92}\text{Ru}$  up to an excitation of about 3.6 MeV. In addition it predicts the existence of several other states in this energy region. A similar good agreement is also observed in the case of  $^{90}\text{Mo}$ . Thus, as may be seen in fig. 4, the calculation accounts for all observed states of this nucleus up to about 3 MeV of excitation and for most levels the difference between observed and calculated excitation energy does not exceed 300 keV.

The results of the calculation on the electromagnetic properties of the  $Z, N \leq 50$  nuclei are summarized in table 2. As may be observed in this table, the predictions of the calculation are, generally, in impressive agreement with the experimental data. Such a feature certainly increases the confidence on the validity of the model employed in the calculation.

Using the wavefunctions of the calculation we have also calculated double  $\beta$  matrix elements for the Ge, Se, Kr and Sr isotopes. A detailed description of this calculation may be found in Ref. 13, where also the results of our calculation are compared with the Los Alamos<sup>15)</sup> predictions with which they are found, generally, to be in agreement. Table 3 shows a sample of these results, namely the matrix elements for the  $^{76}\text{Ge} \rightarrow ^{76}\text{Se}$  transition. These matrix elements are shown for all operators

**Table 2**  
Reduced Transition Probabilities  $B(QL)$  in the  $Z, N \leq 50$  nuclei

$QL$	Nucl.	$J_i^\pi$	$E_i^\dagger$	$J_f^\pi$	$E_f^\dagger$	Exper. $^\dagger$	Calc. $^\dagger$
$M1$	$^{92}\text{Mo}$	$2^+$	3091	$2^+$	1509	$0.04 \pm 0.01$	0.05
	$^{89}\text{Y}$	$3/2^-$	1507	$1/2^-$	0	$0.31 \pm 0.02$	0.22
	$^{89}\text{Zr}$	$3/2^-$	1743	$1/2^-$	588	$(32^{+7}_5) \times 10^{-3}$	$7 \times 10^{-3}$
		$23/2^+$	3576	$21/2^+$	2995	$0.13^{+0.13}_{-0.07}$	0.09
		$25/2^+$	4277	$23/2^+$	3576	$\simeq 1.0$	0.89
$E2$	$^{88}\text{Zr}$	$2^+$	1818	$2^+$	1057	$0.15 \pm 0.06$	0.23
	$^{95}\text{Rh}$	$21/2^+$	2449	$17/2^+$	2068	$1.27 \pm 0.20$	5.74
		$6^+$	2498	$4^+$	2187	$0.11 \pm 0.01$	0.20
	$^{94}\text{Ru}$	$8^+$	2645	$6^+$	2498	$(35 \pm 4) \times 10^{-4}$	0.08
		$11^-$	4489	$9^-$	4198	$3.00 \pm 0.60$	8.92
		$12^+$	4717	$10^+$	3992	$3.16 \pm 0.27$	2.99
		$21/2^+$	2534	$17/2^+$	2185	$2.57 \pm 0.01$	2.16
	$^{93}\text{Tc}$	$17/2^-$	2185	$13/2^-$	2146	$0.45 \pm 0.04$	0.67
		$2^+$	1509	$0^+$	0	$9.27 \pm 1.57$	5.99
	$^{92}\text{Mo}$	$6^+$	2612	$4^+$	2283	$3.11 \pm 0.10$	2.87
		$8^+$	2760	$6^+$	2612	$1.28 \pm 0.05$	1.09
		$11^-$	4486	$9^-$	4252	$3.37 \pm 0.20$	3.19
		$9/2^-$	1791	$5/2^-$	1187	$\leq 7.16$	6.11
	$^{91}\text{Nb}$	$13/2^-$	1984	$9/2^-$	1791	$2.86 \pm 0.13$	4.03
		$17/2^-$	2035	$13/2^-$	1984	$1.29 \pm 0.08$	1.61
		$2^+$	2186	$0^+$	0	$5.51 \pm 0.49$	5.42
	$^{90}\text{Zr}$	$2^+$	2186	$0^+$	1761	$6.12 \pm 0.53$	7.60
		$2^+$	3309	$0^+$	0	0.65	1.16
		$6^+$	3448	$4^+$	3077	$2.47 \pm 0.10$	7.08
		$2^+$	3843	$0^+$	0	1.98	0.57
		$3/2^-$	1507	$1/2^-$	0	$2.80 \pm 0.40$	1.04
	$^{89}\text{Y}$	$5/2^-$	1744	$1/2^-$	0	$2.79 \pm 0.20$	1.75
		$2^+$	1836	$0^+$	0	$7.20 \pm 0.22$	8.79
	$^{88}\text{Sr}$	$2^+$	3218	$2^+$	1836	$0.12 \pm 0.06$	0.05
		$5^-$	3585	$3^-$	2734	$0.39 \pm 0.11$	1.61
		$2^+$	1565	$0^+$	0	$12.1 \pm 1.0$	12.4
	$^{92}\text{Ru}$	$8^+$	2840	$6^+$	2672	$1.70 \pm 0.2$	4.48
	$^{90}\text{Mo}$	$8^+$	2876	$6^+$	2815	3.23	9.30
	$^{89}\text{Zr}$	$9/2^+$	1511	$9/2^+$	0	$< 14$	2.23
		$5/2^+$	1627	$9/2^+$	0	$6 \pm 1$	11.8

Table 2 Continued

<i>QL</i>	Nucl.	$J_i^\pi$	$E_i^\dagger$	$J_f^\pi$	$E_f^\dagger$	Exper. $^\ddagger$	Calc. $^\ddagger$
<i>E2</i>	$^{89}\text{Zr}$	$21/2^+$	2995	$17/2^+$	2724	$3.10^{+0.10}_{-0.09}$	2.83
		$23/2^+$	3576	$21/2^+$	2995	$40^{+5}_{-30}$	9.67
		$3/2^-$	1743	$1/2^-$	588	$0.6^{+0.6}_{-0.4}$	1.24
		$13/2^+$	1944	$9/2^+$	0	$1.2 \pm 0.2$	8.78
		$17/2^+$	2724	$13/2^+$	1944	$7^{+3}_{-2}$	10.9
	$^{88}\text{Zr}$	$2^+$	1057	$0^+$	0	$22 \pm 7$	13.8
		$2^+$	1818	$2^+$	1057	$2.1 \pm 0.9$	8.32
		$8^+$	2887	$6^+$	2810	$1.75 \pm 0.3$	7.71
	$^{86}\text{Sr}$	$2^+$	1077	$0^+$	0	$10.5 \pm 1.4$	11.6
		$8^+$	2956	$6^+$	2857	$2.87 \pm 0.19$	6.62
<i>M2</i>	$^{89}\text{Zr}$	$13/2^-$	2121	$9/2^+$	0	$(16^{+8}_{-7}) \times 10^{-4}$	$7 \times 10^{-4}$
<i>E3</i>	$^{90}\text{Zr}$	$3^-$	2748	$0^+$	0	$31.7 \pm 0.81$	14.4
		$8^+$	3589	$5^-$	2319	$0.06 \pm 0.01$	0.11
	$^{89}\text{Y}$	$5/2^+$	2222	$1/2^-$	0	$17.8 \pm 1.56$	16.2
		$7/2^+$	2530	$1/2^-$	0	$18.9 \pm 1.45$	4.37
	$^{88}\text{Sr}$	$2^+$	3218	$3^-$	2734	$22.6 \pm 0.12$	0.10
	$^{89}\text{Zr}$	$13/2^-$	2121	$9/2^+$	0	$1.3^{+0.2}_{-0.3}$	0.83
	$^{88}\text{Y}$	$1^+$	393	$4^-$	0	$5.9 \pm 0.6$	0.48
		$8^+$	675	$5^-$	231	$6 \times 10^{-3}$	$7 \times 10^{-3}$
	<i>M4</i>	$^{95}\text{Rh}$	$1/2^-$	$9/2^+$	0	44.8	109
		$^{93}\text{Tc}$	$1/2^-$	$9/2^+$	0	34.2	87.1
		$^{91}\text{Nb}$	$1/2^-$	$9/2^+$	0	19.0	68.9
		$^{89}\text{Y}$	$9/2^+$	$1/2^-$	0	3.94	11.6
	$^{89}\text{Zr}$	$1/2^-$	588	$9/2^+$	0	$11.4 \pm 0.4$	60.8

 $^\dagger$  In KeV $^\ddagger$  In Weisskopf units

considered in the calculation of Ref. 13.

**Table 3**  
 $\beta\beta$  elements for the  $^{76}\text{Ge} \rightarrow ^{76}\text{Se}$  transition

Operator	Present	Los Alamos
$-Y \cdot Y$	3.90	2.56
$\Omega_\nu$	6.96	4.61
$\Omega_s J_L \cdot J_R$	-2.67	-1.96
$\Omega_s J_L \cdot J_L$	11.5	7.38
$\Omega_t J_L \cdot J_R$	-4.03	-3.05
$\Omega_t J_L \cdot J_L$	6.96	4.61
$\Omega_A$	6.56	3.12
$\Omega_N$	173	190
$\Omega_\Delta$	81	
$\Omega(\text{SUSY})$	-246	

### References

1. J. Sinatkas, L.D. Skouras, D. Strottman and J.D. Vergados, *A study of the  $N = 50$  nuclei*, to be published
2. J. Sinatkas, L.D. Skouras, D. Strottman and J.D. Vergados, *A study of the  $N = 49-48$  nuclei*, to be published
3. I. Talmi and I. Unna, Nucl. Phys. **19**, 225 (1960)
4. S. Cohen, R.D. Lawson, M.H. MacFarlane and M. Soga, Phys. Lett. **10**, 195 (1964)
5. N. Auerbach and I. Talmi, Nucl. Phys. **64**, 458 (1965)
6. J. Vervier, Nucl. Phys. **75**, 17 (1966)
7. J.B. Ball, J.B. McGrory and J.S. Larsen, Phys. Lett. **B41**, 581 (1972)
8. D.H. Gloekner and F.J.D. Serduke, Nucl. Phys. **A220**, 477 (1974)
9. F.J.D. Serduke, R.D. Lawson and D.H. Gloekner, Nucl. Phys. **A256**, 45 (1976)
10. R. Gross and A. Frenkel, Nucl. Phys. **A267**, 85 (1976)
11. A. Amusa and R.D. Lawson, Z. Phys. **A307**, 33 (1982); **A314**, 314 (1983)

12. Table of isotopes, Edited by C.M. Lederer and V.S. Shirley, (J. Wiley and Sons, Inc (New York) 1978).
13. J. Sinatkas, L.D. Skouras and J.D. Vergados, Phys. Rev. **C37**, 1229 (1988)
14. J.P. Elliott, A.D. Jackson, H.A. Mavromatis, E.A. Sanderson and B. Singh, Nucl. Phys. **A121**, 241 (1968)
15. W.C. Haxton, G.J. Stephenson and D. Strottman, Phys. Rev. Lett. **57**, 3148 (1981); Phys. Rev. **D25**, 2360 (1982)